MEASUREMENTS OF THE PROPERTIES OF THE Υ FAMILY FROM e^+e^- ANNIHILATION

Hinrich Meyer
University of Wuppertal, Gauss-Str. 20, 56 Wuppertal 1, Germany

Summary

Information on Υ particles from e^+e^- annihilation experiments at DORIS is summarized. The mass differences in the Υ family as well as the coupling to lepton pairs is found to be very similar to the ψ family. The charge of the constituent b quark is established to be 1/3. The event structure reveals non trivial correlations between the decay particles. The three-gluon decay hypothesis assuming spin 1 gluons provides a quantitative explanation of the data. Gluon jets are found to be rather similar to quark jets for jet energies up to ~ 5 GeV.

Introduction

Information on the properties of the Υ family from e^+e^- annihilation comes from experiments at the e^+e^- storage ring DORIS. The data were taken about a year ago by three collaborations: DASPII (DESY-Dortmung-Heidelberg-Lund), DHHM (DESY-Hamburg-Heidelberg-München) and PLUTO (Aachen-DESY-Hamburg-Siegen-Wuppertal). The experiments were made possible by a great effort of the DORIS storage ring group to operate the e^+e^- ring at energies much higher than originally foreseen [1].

In the first running period in April - May 1978 at total energies more than 9.0 GeV DASPII [2] and PLUTO [3] obtained resonance signals corresponding to the Υ(9.46) as shown in fig. 1. PLUTO then left the south interaction region of DORIS to be ready for first measurements at PETRA and was replaced by the DESY-Heidelberg detector. The Υ(9.46) was confirmed in June 1978 and finally in August 1978 [4,5] the Υ' (10.02) was detected, fig. 2.

1. Parameters of the Υ Particles

From the resonance signals several interesting parameters have been determined, the masses, the partial width Γ_{ee}, the hadronic width Γ_{had} and the charge of the constituent quark. The resonance signal at mass M with total width Γ_{tot} and hadronic width Γ_{had} is given by

$$\sigma_{res} = \frac{12\,\pi\,M^2}{S}\;\frac{\Gamma_{had}\,\Gamma_{ee}}{(S - M^2)^2 + M^2\,\Gamma_{tot}}$$

with $S = 4\,E_0^2$ is the total center of mass energy squared. A single parameter is determined, Γ_{ee}, the partial width to e^+e^- pairs, if

$$\Gamma_{had} \gg \Gamma_{ee}.$$

The observed width of the Υ(9.46), σ = 7.3 MeV, and of the Υ'(10.02), σ = 11 MeV, is due to the finite energy spread of the e^+e^- beams in DORIS and compatible with values calculated from the e^+e^- beam dynamics.

Radiation of photons in the initial stage strongly reduces the resonance signal, in case of Υ(9.46) at DORIS by a factor of about 1/0.63. The values for Γ_{ee} obtained are shown in table 1. The mass determinations are dominated by the uncertainty in absolute energy calibration of the DORIS ring, about 10 MeV at the Υ(9.46) and 20 MeV at the Υ'(10.02). The much larger uncertainty at 10 GeV as compared to 9.5 GeV results from strong saturation effects in the DORIS magnets near the end of the accessible energy range.

Using the masses of the Υ(9.46) and Υ'(10.02) as input it was possible from the high resolution data of

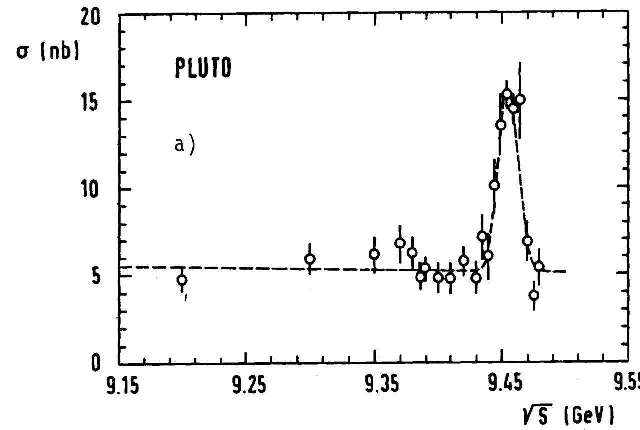

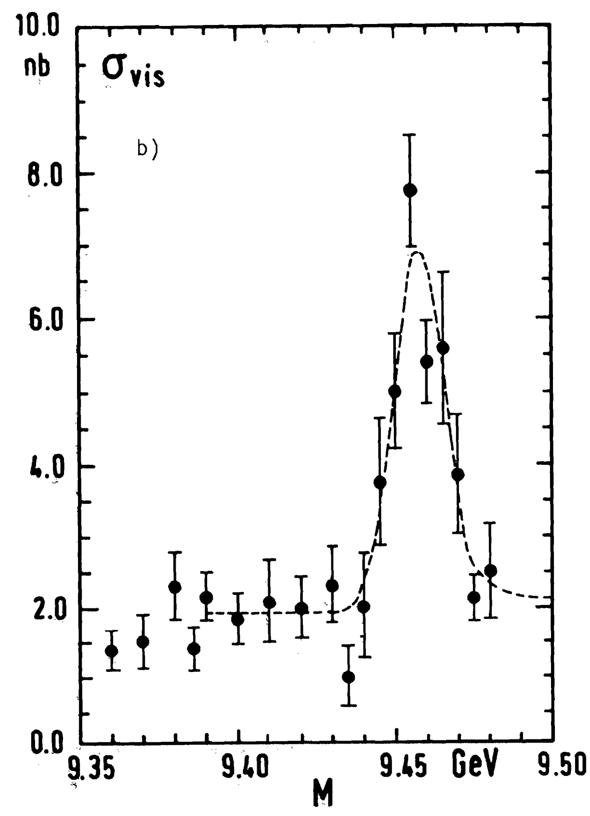

Fig. 1 The Υ(9.46) signals from
a) PLUTO and
b) DASPII.

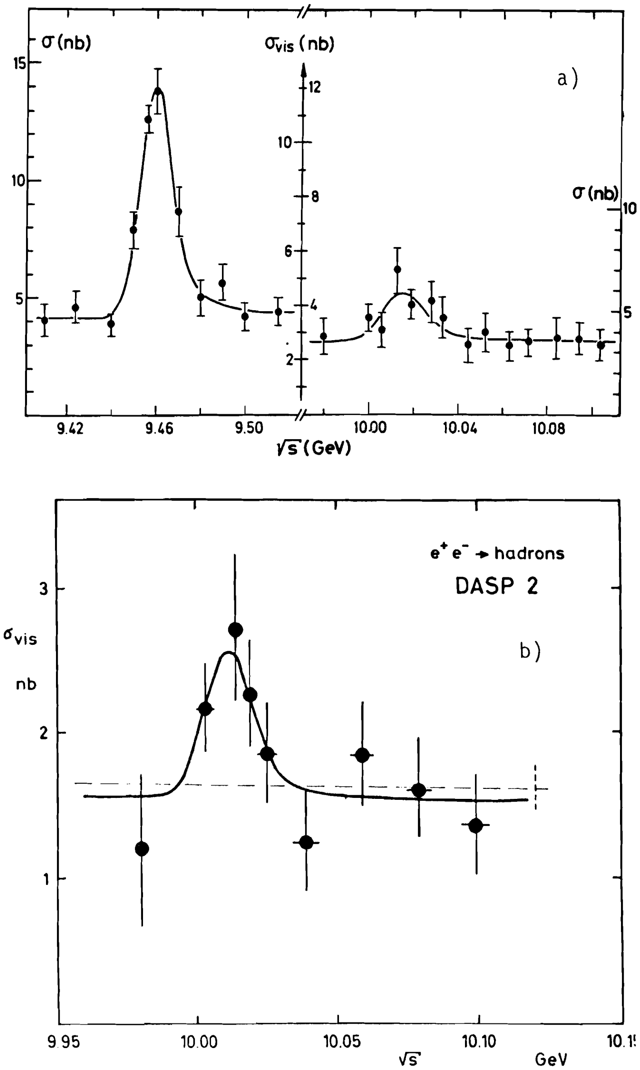

Fig. 2 The Υ(9.46) and Υ'(10.02) signal as
a) seen by DHHM and
b) the Υ'(10.02) from DASPII.

Table 1

Experiment	Ref.	Mass(GeV)	Γ_{ee} (KeV)	$B_{\mu\mu}$ (%)	σ (MeV)
PLUTO	15	9.456 ± 0.01	1.33 ± 0.14	2.2 ± 2.0	7.3 ± 0.1
DHHM	4,17	9.46 ± 0.01	1.04 ± 0.28	$1.0 {+3.4 \atop -1.0}$	7.1 ± 0.8
DASP 2	2,16	9.457 ± 0.01	1.50 ± 0.40	2.5 ± 2.1	7.6
Mean values		9.46 ± 0.01	1.28 ± 0.27	2.1 ± 1.4	
DHHM	4	10.02 ± 0.02	0.32 ± 0.13		12 ± 4
DASP 2	5	10.012 ± 0.02	0.35 ± 0.14		9
Mean values		10.015 ± 0.02	0.33 ± 0.14		

the collaboration here at Fermilab [6] to establish the existence of a Υ" at a mass of 10.41 ±0.05 GeV, see fig. 3. It leads to the level scheme for the Υ family sketched below and compared to the ψ family. The Υ"(10.41) waits for observation in e^+e^- annihilation

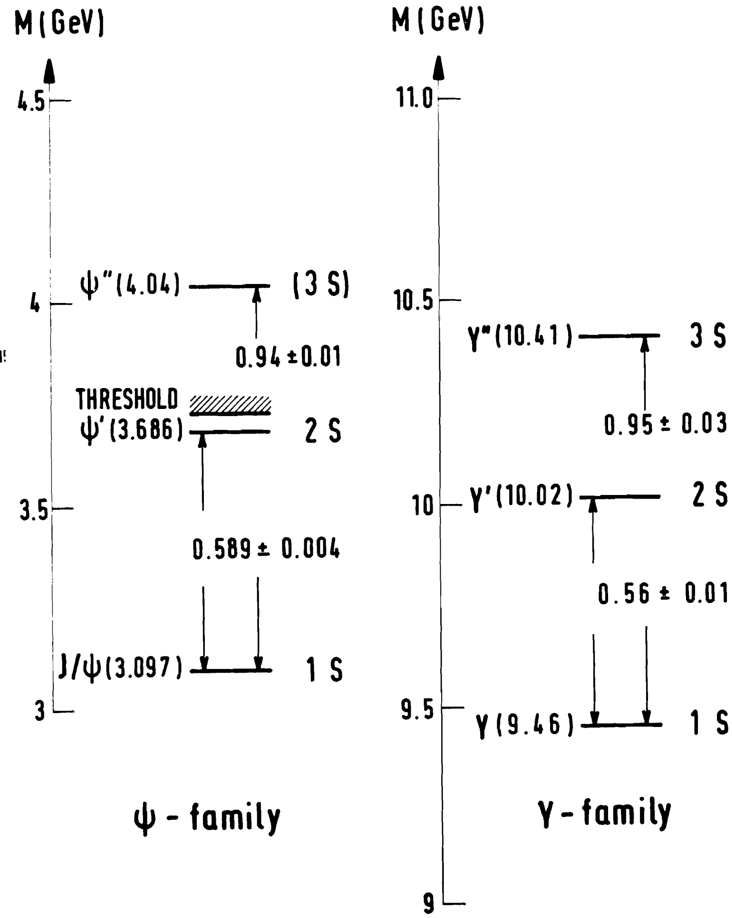

experiments as well as the detection of the threshold for the new 'B particles', probably at energies just above the Υ"(10.41) mass. A signal recently observed in the ψKπ final state at a mass of 5.30 GeV may be taken as evidence for the B particles [7]. It would place the threshold at an energy of 10.60 GeV.

A very detailed study of quark-antiquark binding potentials by Quigg, Rosner and Thacker [8] allows a de-

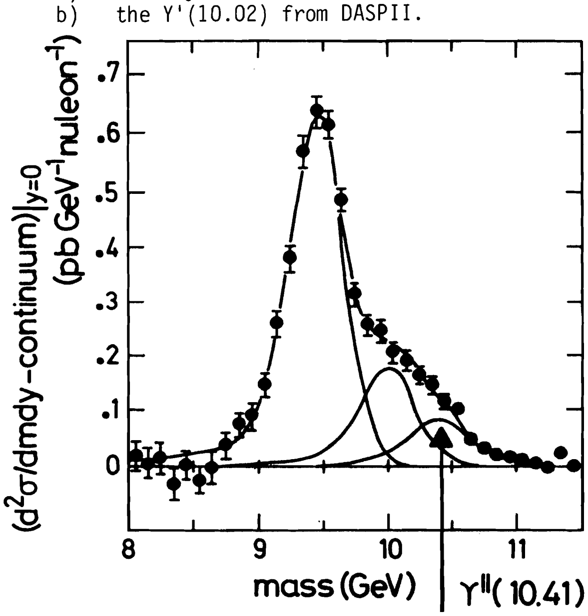

Fig. 3 High resolution data in $M_{\mu^+\mu^-}$ from ref. 6 for the reaction $p + N \to \mu^+ \mu^- +$ anything.

termination of the quark charge from the measured width of Υ(9.46) and Υ'(10.02) to e^+e^- pairs. Fig. 4 illustrates the result based on the average of the values for Γ_{ee} from table 1, clearly the charge assignment 1/3 is favoured.

Recent data from PETRA on the total annihilation cross section confirm this conclusion. The sum rule for σ_{tot} including first and second order QCD corrections reads[9,10]

$$R = \frac{3S}{4\pi\alpha^2}\sigma_{had} = 3\sum_i (e_{q_i})^2 \times$$

$$\left[1 + \frac{\alpha_s}{\pi} + (1.98 - 0.116\, N_f)\left(\frac{\alpha_s}{\pi}\right)^2\right]$$

where e_{q_i} are the quark charges and N_f is the number of quark flavours. From u, d, s, c quarks we get an asymptotic (α_s/π very small) value of 10/3, a b(1/3) adds 1/3 while a b(2/3) will add 4/3. Higher order corrections to R including calculations to second order in α_s/π are small, less than 7 % for a value $\alpha_s = 0.2$. Fig. 5 shows data from the PLUTO collaboration in the range 3.6 GeV < E_{CM} < 31.6 GeV, with the contribution from the τ lepton subtracted. The average value of R above 13 GeV is 3.88 ±0.22 (±15 %) in good agreement with the b(1/3) charge assignment. Table 2 summarizes the values for R obtained by the four groups working at PETRA [11 - 14]. The possible systematic scale shifts reported are ~ 10 - 15 %, however, since all four experiments determine the luminosity separately and are rather different in event definition and acceptance corrections the true error on R for the four experiments taken together is probably only ~ 5 %. The b(2/3) charge assignment then is excluded at the 6 standard deviation levels.

Table 2

Experiment	Ref.	Energy(GeV)	R
PLUTO	11	13 - 31.6	3.88 ± 0.22
JADE	13	22 - 31.6	4.14 ± 0.26
MARK J	12	13 - 31.6	4.11 ± 0.17
TASSO	14	13 - 31.6	3.98 ± 0.20
Mean value			4.03 ± 0.12
Theory	10		3.90

A comparison of the width Γ_{ee} divided by the quark charge squared of the Υ family with the values known for the lower lying vector mesons is given in fig. 6. It suggests a rather constant behaviour with vector meson mass and a ratio of about 2.5 for the values from the ground state (^1S) to the first radial excitation (^2S).

The determination of Γ_{ee} uses the assumption $\Gamma_{had} \gg \Gamma_{ee}$ where Γ_{had} is the decay width of the Υ(9.46) into hadrons. Γ_{had} can be determined from a measurement of a resonance signal in $e^+e^- \to \mu^+\mu^-$. Assuming lepton universality the DORIS groups have attempted to measure $B_{\mu\mu}$ [15 - 17]. The results are summarized in table 1. The uncertainty in $B_{\mu\mu}$ is still so large that the upper limit on Γ_{had} is only the observed width of the Υ(9.46)

$$25 \text{ keV} < \Gamma_{had} < 17000 \text{ keV}.$$

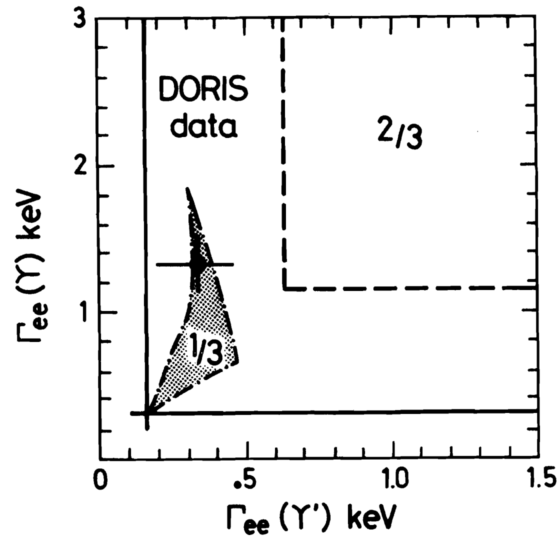

Fig. 4 Lower bounds for $\Gamma_{ee}(\Upsilon)$ and $\Gamma_{ee}(\Upsilon')$ for b-quark charges of 1/3 and 2/3. The shaded area indicates the allowed region for charge 1/3. The data point is from table 1.

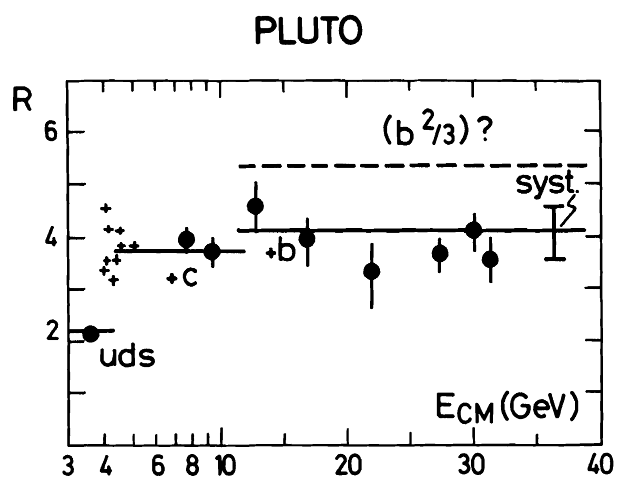

Fig. 5 Data from PLUTO on $\sigma(e^+e^- \to had)$.

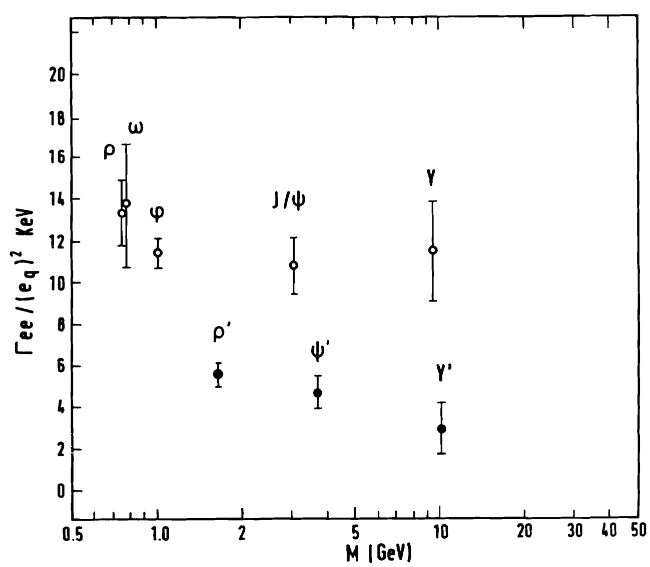

Fig. 6 Leptonic width divided by the quark charge squared for the known vector mesons.

A lower limit on Γ_{had} can also be derived using the event structure on and off resonance (see part 2 below). For the data from the PLUTO collaboration an increase of $B_{\mu\mu}$ above 5 % leads to negative values for the lowest sphericity (thrust, $\sin^2\delta$) bin in fig. 15 and therefore to a lower limit 27 keV < Γ_{had} in good agreement with the value obtained from $B_{\mu\mu}$.

2. Hadronic decays of the Y and Y'

From the results on Γ_{had}, Γ_{ee} and $B_{\mu\mu}$ of the Y(9.46) we know that the electromagnetic contribution to the hadronic Y(9.46) decays, given by

$$\sigma_{Y_\gamma}/\sigma_{res} = R \cdot B_{\mu\mu}$$

is less than ~ 20 %. It is the remaining part of the hadronic Y(9.46) decays that we are interested in and which will be discussed below. The experimental information is extracted as indicated in fig. 7. The signal at resonance contains three contributions

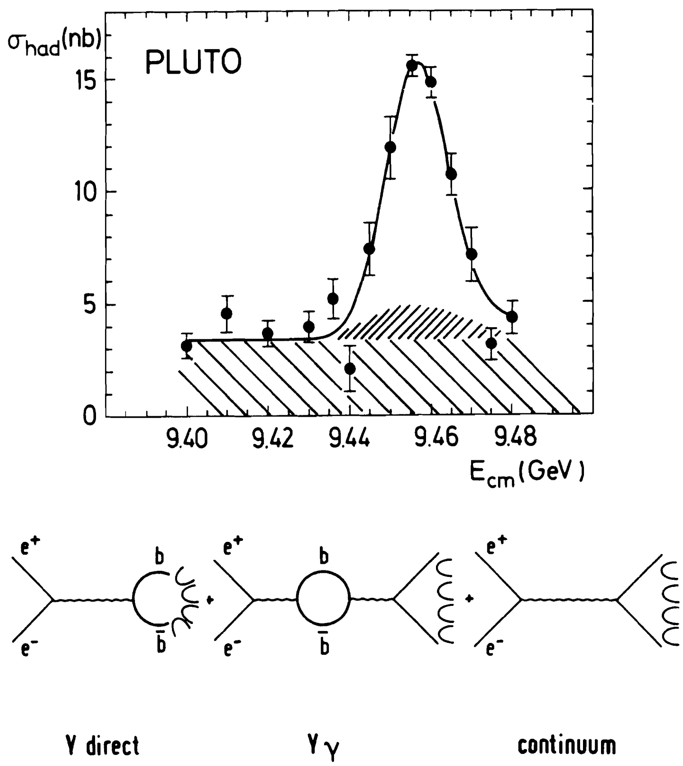

Fig. 7 Y(9.46) resonance signal from ref. 15. The three contributions to it (Y_{direct}, Y_γ and continuum) are shown below and indicated by the shaded area.

the direct resonance decays (Y_{direct}), the vacuum polarization term (Y_γ) and nonresonant contributions (continuum). The second and third parts are identical in final state and are described by data just below resonance, since the energy variation in the final states going from 9.40 GeV to 9.46 GeV can safely be neglected. The main uncertainty is in the value of $B_{\mu\mu}$, however, the conclusions about properties of the hadronic Y(9.46) decays to be discussed below are only weakly dependent on the exact value of $B_{\mu\mu}$.

2.1. Models

The data on $Y_{dir.}$ will be compared to three models, different by the degree of correlation among the final state particles. One extreme is simple phase space, which has no other correlation between the particles than energy and momentum conservation. It provides a one (essentially) parameter comparison since the particle multiplicity has been fixed to correspond to the observed one.

Another extreme with very strong correlations is a two-jet model based on the description by Field and Feynman[18]. It has been extended beyond the original version by including heavy quarks, the charm quark (c) and above $\sqrt{s} \simeq 11$ GeV the b quark. This model is known to give a fairly good fit to experimental data on hadronic jet properties in weak and electromagnetic current induced processes and in particular for the two-jet events in e^+e^- annihilation[19].

However, there is also a very interesting model which supposedly provides a realistic framework for describing the Y(9.46) decay properties. In QCD a heavy quark-antiquark resonance system decays into 3 gluons in lowest order of the running coupling constant

$$\alpha_s = \frac{12\pi}{(33 - 2N_f)\ln S/\Lambda^2} .$$

At Y(9.46) we expect a value for α_s of ~ 0.2. Therefore, it seems not to be unreasonable to persue a model for Y(9.46) decays based on the three-gluon decay matrix element (positronium analogue)[20]

$$\frac{1}{\Gamma}\frac{d\Gamma}{dx_1\,dx_2} = \frac{6}{\pi^2 - 9} \times \left| \frac{x_1^2(1-x_1)^2 + x_2^2(1-x_2)^2 + x_3^2(1-x_3)^2}{x_1^2\,x_2^2\,x_3^2} \right|$$

where x_i are the scaled (massless) gluon momenta, $x_i = E_i(\mathrm{gluon})/E(\mathrm{beam})$ and $x_1 + x_2 + x_3 = 2$. The matrix element is rather flat over the $x_1x_2x_3$Dalitz plot (see fig.24a)with variations of about 20 %. The most fequent final state is two fast gluons $x_1, x_2 \simeq 1$ and $x_3 \ll 1$ while the more spectacular 'mercedes star' structure $x_1 = x_2 = x_3 = 2/3$ is the most unlikely one[20]. The structure of the average three-gluon event for the Y(9.46) drawn to scale is shown below.

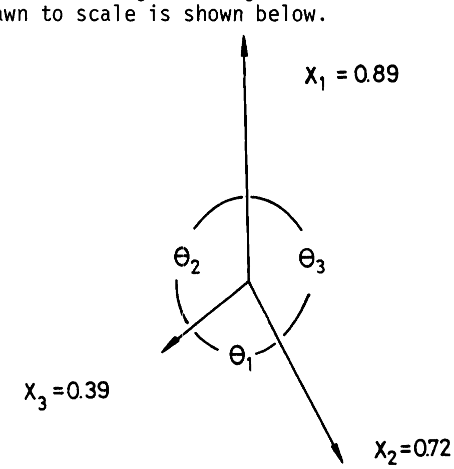

Fig. 8 The structure in momentum space of the average three-gluon event according to the positronium formula (ref. 20).

The fragmentation properties of the gluons have been assumed to be the same as for quarks. This assumption seems plausible since due to insufficient energy of the gluons no long tree with hard quark and gluon vertices can develop before the hadronization stage has been reached. The hadron distributions for each type of jet are certainly dominated by effects at the confinement radius as sketched below.

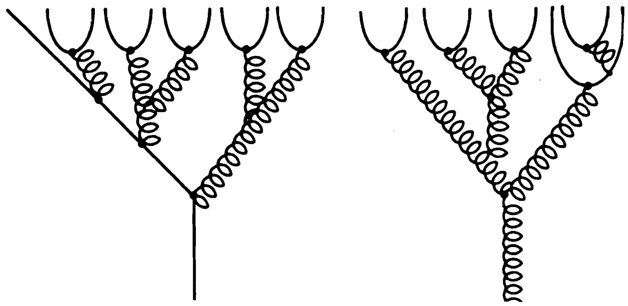

Fig. 9 Fragmentation trees of quarks and gluons at relatively low energy. After at most one hard radiation the confinement level is reached.

2.2. Two-Jet Analysis

The data in the vicinity of the resonances and at higher energies are clearly very well described by a dominant two-jet structure in good agreement with phenomenological parametrizations of quark jets a la Field-Feynman[21]. The Y(9.46) data are not described by a two-jet quark model. This is clearly seen for data from PLUTO using charged and neutral particles to get various measures of 'jettiness' sphericity (SPH)[22], fig. 10, thrust (T)[23], fig. 11, and the average energy weighted opening angle ($\sin^2\delta$)[24], fig. 12. The dotted line shows the result of the Field-Feynman model, and also shown are the values for the phase space and the three-gluon model [25]. The value for phase space is much higher than the Y(9.46) data, while the three-gluon model is very close.

Fig. 13 shows data from DASPII with no subtraction procedure applied[26]. Since only angles and no momenta are measured 'pseudo' quantities have been defined to describe the jet properties. Clearly going across the resonance a change away from two-jet structure is observed.

A more detailed comparison is possible for distributions in sphericity or thrust. Fig. 14 shows the result from DHHM for both Y(9.46) and Y'(10.02) data and for the continuum[27]. Fig. 15 gives distributions from PLUTO.

The results can be summarized as follows:

(a) The continuum data is well described by the quark-jet parametrization from Field-Feynman.

(b) A simple phase space does not give a fit to the data from the Y(9.46).

(c) The three-gluon model certainly is a rather good parametrization of the Y(9.46) (and Y'(10.02)) data.

Two more arguments can be given to support these conclusions. Fig. 16 shows the sphericity (calculated from charged particles only) for different charged particle multiplicity classes[25]. It is seen that the Y(9.46) data is inbetween phase space and the two-jet model by about the same amount for each multiplicity class separately. It shows that essentially all events and not just a subclass from the Y(9.46) are different from the two extremes phase space and two-jet model while there is again good agreement with the three-gluon model. Furthermore, from Fig. 17 we see that the

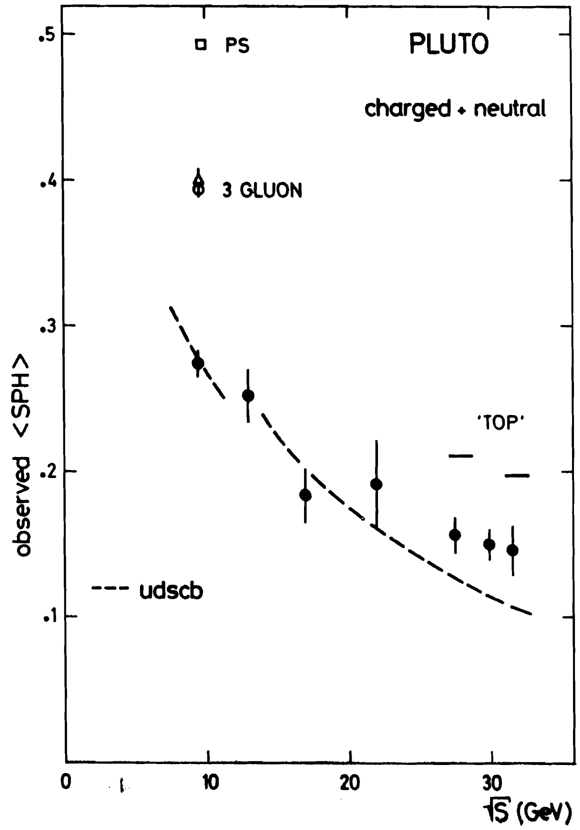

Fig. 10 The average sphericity vs.energy calculated from charged and neutral particles. The dotted line is the result of the Field-Feynman model, PS indicates phase space and 3 gluon the result of a three-gluon model prediction.

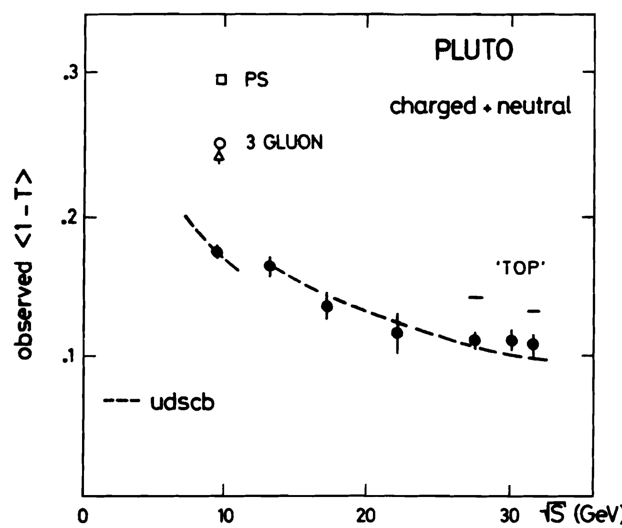

Fig. 11 The average thrust vs.energy, otherwise the same as fig. 10.

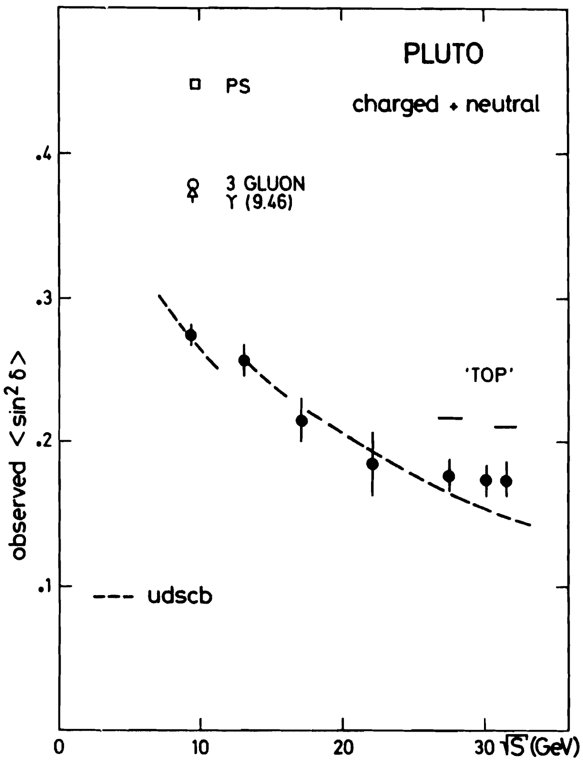

Fig. 12 The average energy weighted opening angle (squared) vs energy, otherwise the same as fig. 10.

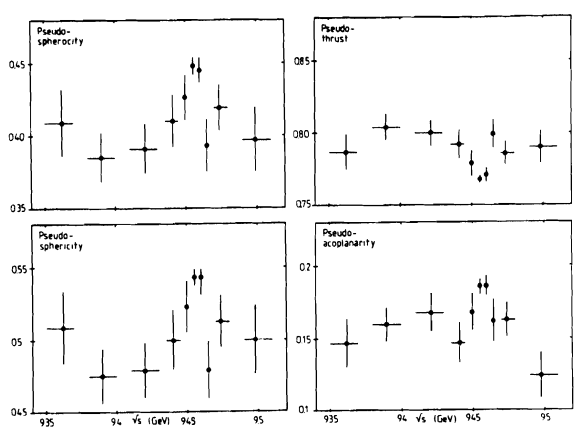

Fig. 13 Various jet quantities, calculated from the observed tracks in DASPII, ref. 26.

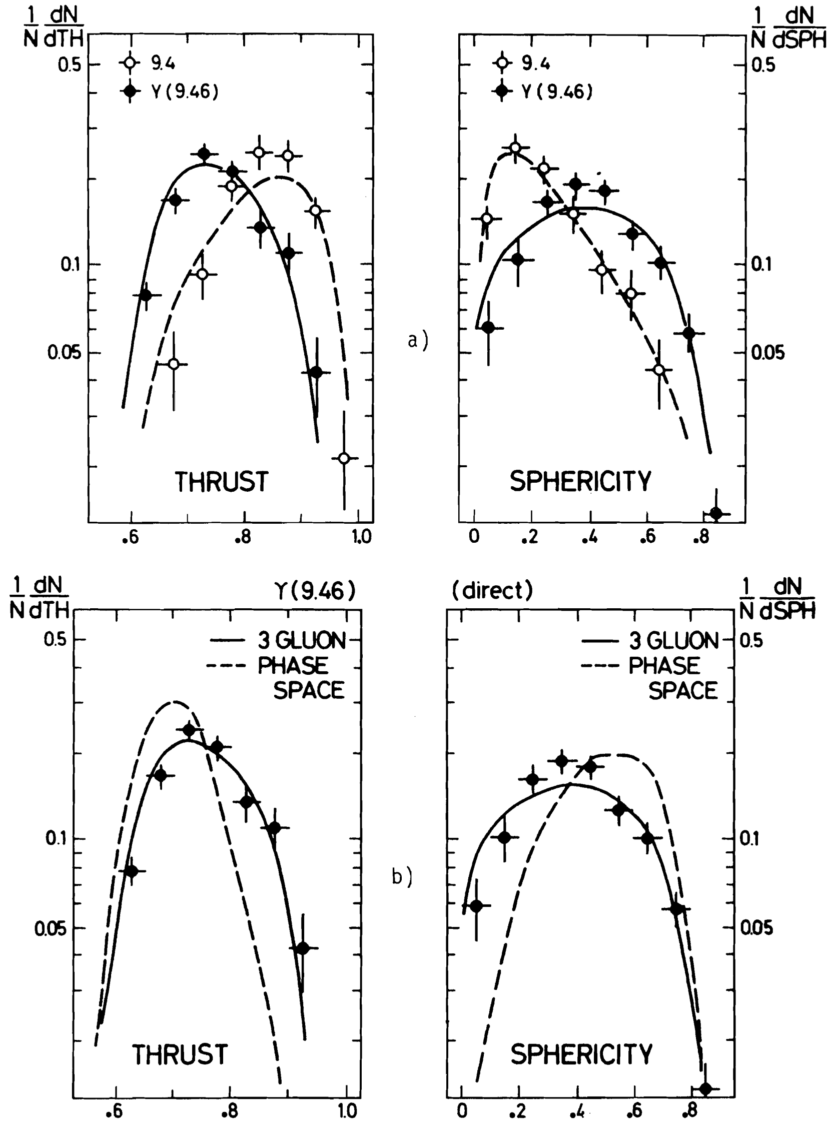

Fig. 15 Sphericity and thrust distributions for
a) Υ(9.46) ♦ and continuum (9.4), ♢ the dashed line is the two-jet model, and for
b) Υ(9.46) ♦ and phase space (dashed line). The full line is the result of the three-gluon model. The data is from PLUTO.

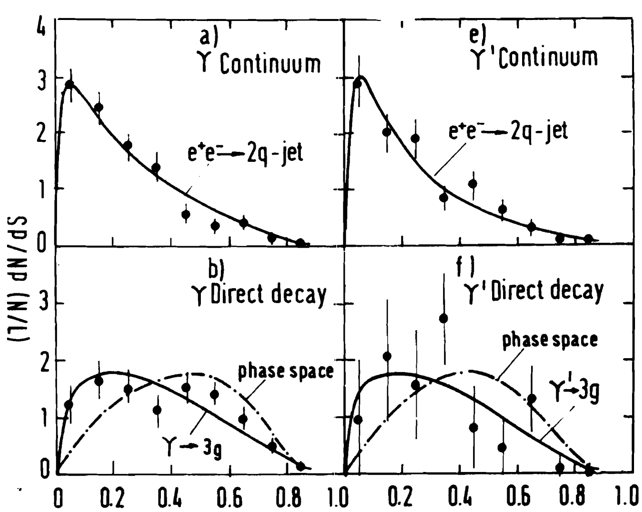

Fig. 14 Sphericity distributions for the Υ(9.46). Υ'(10.02) and the nearby continuum from ref. 27. For comparison the results from two-jet, three-gluon jet and phase-space calculations.

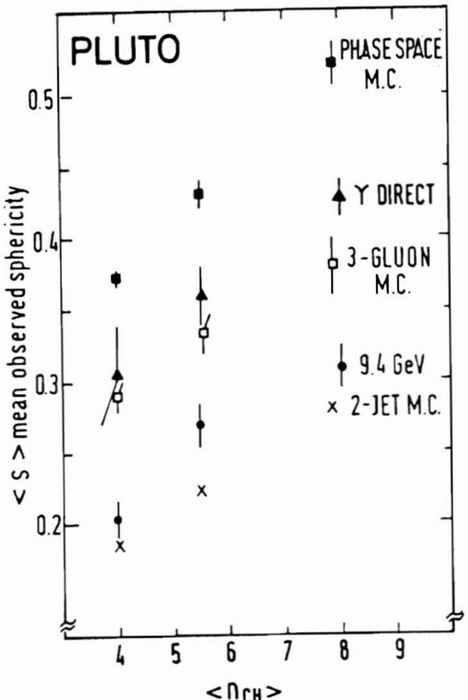

Fig. 16 Average sphericity (charged particles) for various multiplicity classes from ref. 25.

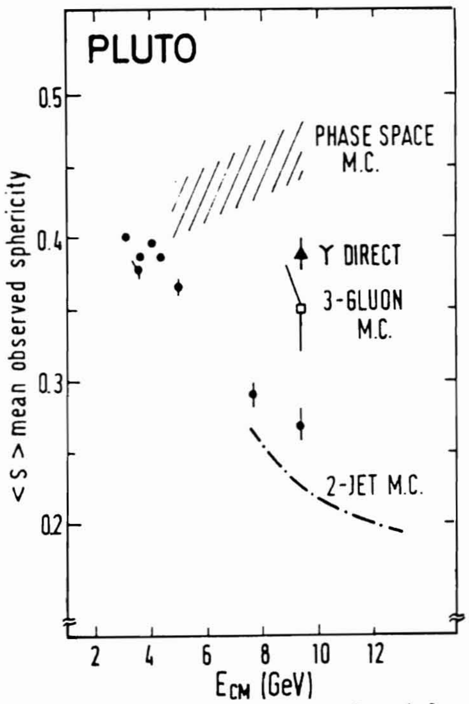

Fig. 17 Average sphericity calculated from charged particles only $\sqrt{s}$ energy, ref.25.

sphericity values for the Υ(9.46) and the J/ψ(3.1) are about the same and in addition the values from phase space and at 3.6 GeV are very close to the J/ψ(3.1) value[25]. Going to higher energies the sphericity of phase space has to rise irrespective of the details of the phase space model just from the increase in particle multiplicity. It is found, however, that the sphericity of Υ(9.46) is significantly lower than phase space for the same multiplicity. This shows in a model indipendent way that one finds experimentally nontrivial momentum correlations at Υ(9.46). In the three-gluon model this is due to the structure of the three-gluon matrix element which predicts three-gluon jets[20]. The gluon fragmentation properties are taken similar to quark fragmentation resulting in a very good agreement for Υ(9.46) decay data and the three-gluon model.

Finally the fact that the sphericity on Υ(9.46) is higher than the two-quark jet data just off resonance excludes 'black box' models in general, where the $b\bar{b}$ system turns into two light quarks as sketched below.

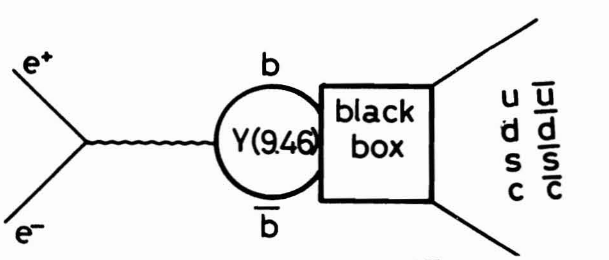

Fig. 18 Possible transitions of the $b\bar{b}$ resonance into low mass quark pairs.

2.3. Three-Jet Analysis

The success of the three-gluon model using measures of two jettiness calls for a three-jet analysis. The PLUTO collaboration has used a three-jet quantity (Triplicity) defined analoguous to collinear thrust[28]. The final state hadrons with the momenta $\vec{p}_1 \dots \vec{p}_N$ are grouped into 3 non empty classes C_1, C_2, C_3 with the total momenta $\vec{P}(C_l) = \Sigma \vec{p}_i$, $i = 1, 2, 3$, $i \in C_l$. Triplicity T_3 is then defined by

$$T_3 = \left(1 \Big/ \sum_{i=1}^{N} |p_i|\right) \max_{C_1,C_2,C_3} |\vec{P}(C_1)| + |\vec{P}(C_2)| + |\vec{P}(C_3)|$$

The limiting values are

$$3 \cdot \sqrt{3}/8 < T_3 < 1 .$$

Momentum conservation puts the three-jet vectors into a plane. One gets two equivalent Dalitz plots having either $x_1 < x_2 < x_3$ the three-jet energies or the $\theta_1 < \theta_2 < \theta_3$, the angles between the three jets (see fig. 8). The ordering of x_i, θ_i reduces the large triangle to the small one, fig. 19, and the characteristic event structures are indicated for the three-corners of the triangles[29].

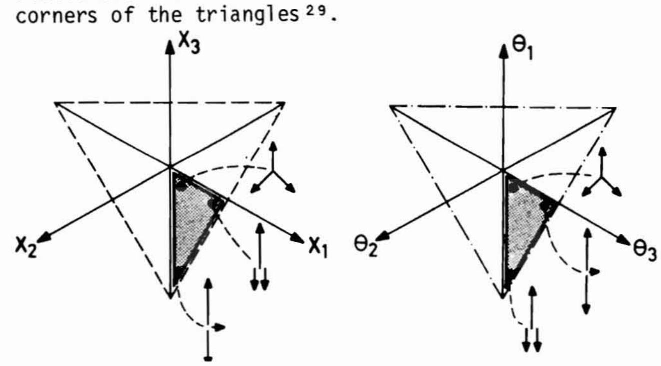

Fig. 19 Event structures in x_i and θ_i as defined in fig. 8.

Projections of the event density in the triangles on x_1, x_3, fig. 20, and on θ_1, θ_3, fig. 21, are compared to the three-gluon model. The agreement again is very good. For comparison phase space is shown (dotted line) again to demonstrate that phase space is still not very much separated from the three-gluon model at this low energy although quantitatively it is not a description for the Υ(9.46) data.

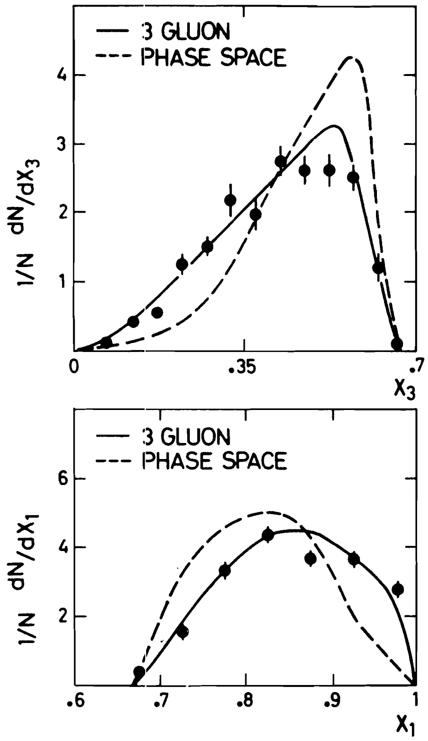

Fig. 20 Results of the triplicity analysis for x_1, x_3 on Υ(9.46) and compared to the three-gluon model (full line) and phase space (dashed line).

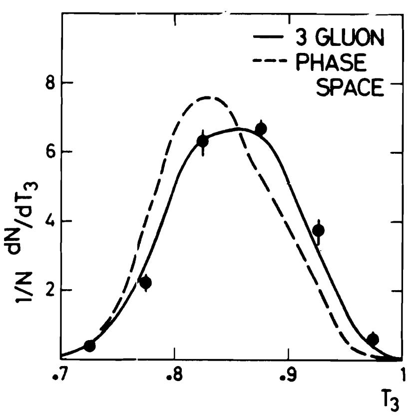

Fig. 22 The triplicity distribution on Υ(9.46).

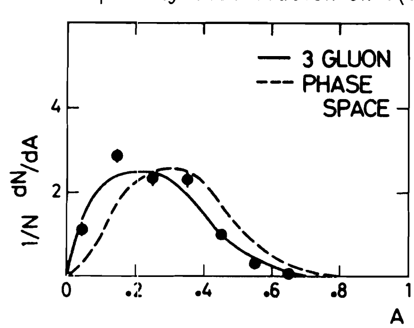

Fig. 23 The aplanarity distribution on Υ(9.46).

The triplicity (T_3) distribution alone does not give a very strong discrimination against phase space, see fig. 22. This holds true also for the aplanarity[28], fig. 23.

Table 3 shows average values for three jet quantities for the PLUTO analysis of the Υ(9.46) in compari-

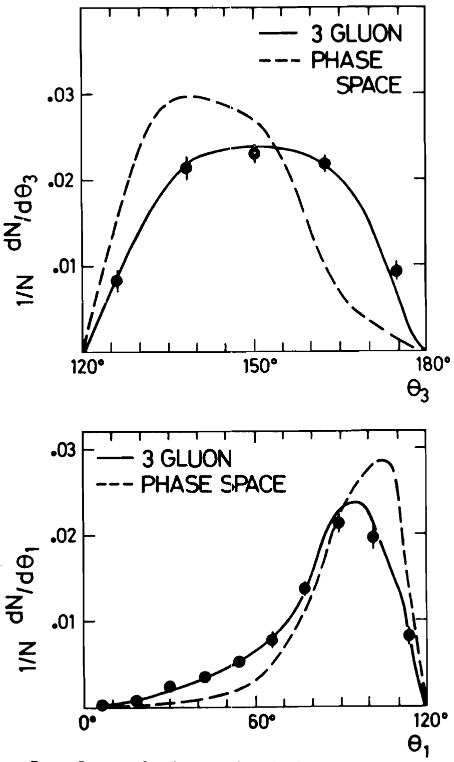

Fig. 21 Results of the triplicity analysis for θ_1, θ_3 on Υ(9.46), otherwise as in fig. 21.

son to the phase space and the three-gluon model. The off resonance data has also been analyzed resulting in sufficiently different distributions in θ_1, θ_3 and x_1, x_3 (not shown)[28].

Table 3

Υ (9.46)

Model Comparision

	Υ Direct data	3-Gluon MC	Phase Space MC
$< T >$	0.715 ± 0.004	0.712 ± 0.003	0.671 ± 0.003
$< T_3 >$	0.858 ± 0.002	0.850 ± 0.002	0.838 ± 0.002
$< x_1 >$	0.855 ± 0.004	0.853 ± 0.003	0.819 ± 0.002
$< x_2 >$	0.722 ± 0.004	0.724 ± 0.003	0.700 ± 0.002
$< x_3 >$	0.423 ± 0.006	0.422 ± 0.005	0.481 ± 0.004
$< \theta_1 >$	84.1° ± 1.0°	85.5° ± 0.8°	93.2° ± 0.6°
$< \theta_2 >$	125.6° ± 0.7°	124.3° ± 0.5°	122.9° ± 0.4°
$< \theta_3 >$	150.3° ± 0.6°	150.2° ± 0.5°	144.0° ± 0.4°

The three-jet analysis does not prove, however, the existence of three-jet structure unambiguously since possibly other more arbitrary final-state configurations can be constructed which numerically agree with the result of this analysis. However, the agreement demonstrated with the numbers summarized in table 3 is most likely not accidental and can be taken as strong support of the three-gluon decay hypothesis for the Υ(9.46).

3. Gluon Spin

The analysis of the Υ(9.46) decay structure reveals quantitative agreement with the three-gluon decay matrix element. It is calculated for massless spin 1 gluons. The data therefore support the spin 1 assignment to the gluon. A natural question then is, can the data be described by spin 0 gluons as well? Koller and Krasemann have provided an expression for a three-gluon matrix element with spin 0 gluons[30].

$$\frac{1}{\Gamma}\ \frac{d\Gamma}{dx_1dx_2} = \frac{1}{\ln M/\Delta} * \frac{(x_1 - x_2)(x_3 - x_2)(x_1 + x_3 - x_2)+\text{even perm.}(1,2,3)}{x_1^2\ x_2^2\ x_3^2}$$

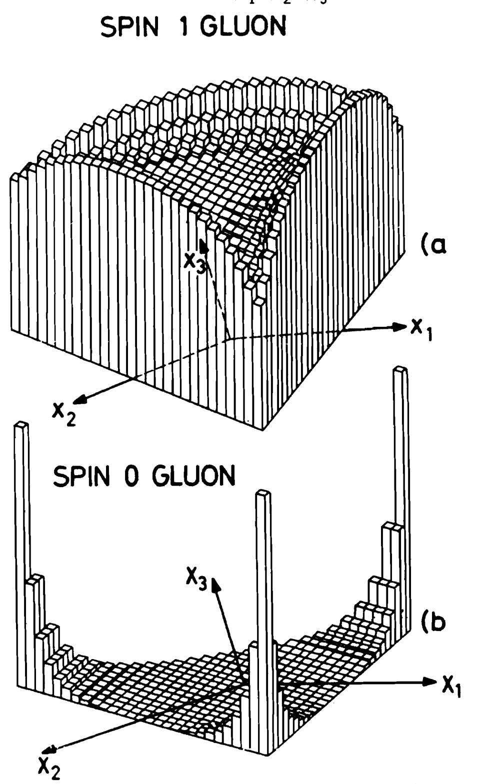

Fig. 24 Graphical representation of the three-gluon matrix element for
a) spin 1 and b) spin 0 from ref. 30.

Fig. 24 shows the Dalitz plot density distribution for spin 1 and spin 0. In the spin 0 case there is a peaking in the corners of the triangle. The corners correspond to $x_1 = x_2$, $x_2 = x_3$ and $x_2 = x_1$ and the final state is dominantly two gluons of about equal energy and the third one with very little energy. It follows that one should expect a dominant two-jet structure. This is not supported by the data and provides a falsification of the spin 0 case. Spin 1 does, however, not necessarily follow . Although the true spin 1 gluon matrix element is in good agreement with the data any phase space like distribution of three low mass clusters will give a very similar distribution[31]. The analogue of this statement was already observed by Ore and Powell in their paper[32] on the three-photon decay of positronium.

For a positive spin 1 determination a measurement of the angular distribution of the fastest gluon (x_1 in fig. 8) with respect to the e^+ beam axis is most appropriate[33].The general form is

$$d\sigma/d\cos\theta = A + B(x_1)\cos^2\theta.$$

$B(x_1)$ is shown in fig. 25. The statistics of the data samples in the DORIS experiments is not sufficient for such a detailed comparison. Integration over the probability distribution for x_1 predicts for the coefficient of $\cos^2\theta$ a value of 0.39. The spin 0 case, however, gives -0.995[30]. The data is shown in fig. 26[25]. While spin 0 again is excluded by the data only consistency with a value 0.39 can be seen, not an unambiguous determination. It should be remarked here that this analysis is sensitive to the exact value of $B_{\mu\mu}$, since the continuum and the vacuum polarisation term have a value ~ 1 for the coefficient of $\cos^2\theta$.

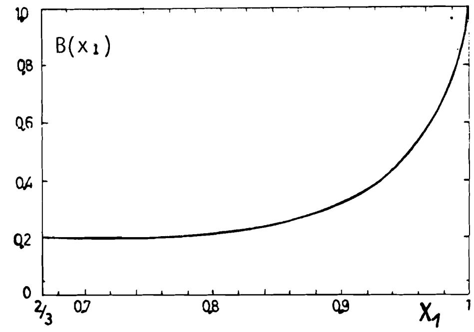

Fig. 25 The coefficient $B(x_1)$ vs x_1 for a spin 1 three-gluon decay of the Υ(9.46) (see text).

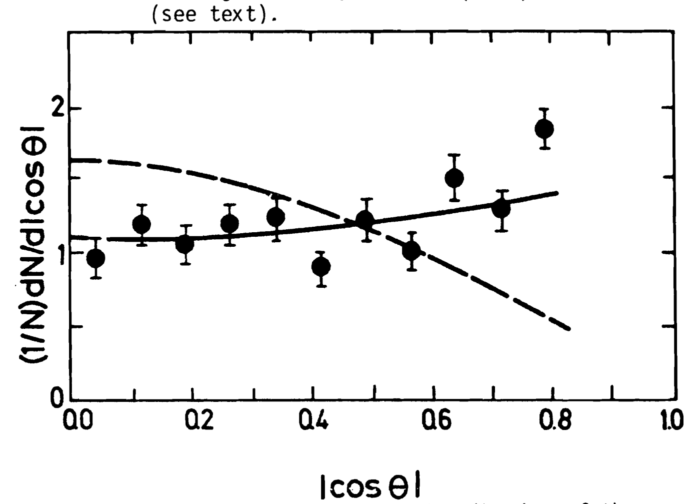

Fig. 26 Data on the angular distribution of the sphericity axis (for charged sphericity) with the beam and compared to the predictions for spin 1 (full line) and spin 0 (dashed line), refs.25 and 30..

While it seems rather unsatifactory to try to construct a Υ(9,46) decay model based on spin 0 gluons in the first place, it is gratifying to see the one model actually worked out in detail to be falsified[30]. Spin 1 on the other hand remains to be proven.

4. Fragmentation Properties of the Gluon

There are several specific features of the gluon that should reflect into the properties of the gluon jets and make them different from quark jets[31].

(a) The gluon should fragment softer which means with higher multiplicity than a quark jet, asymptotically by a factor 9/4.

(b) In addition the average $<p_\perp>$ of hadrons with respect to the gluon-jet axis should be broader.

Both a and b are due to the existence in QCD of a gluon selfcoupling, the three-gluon vertex, the most

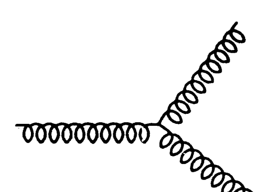

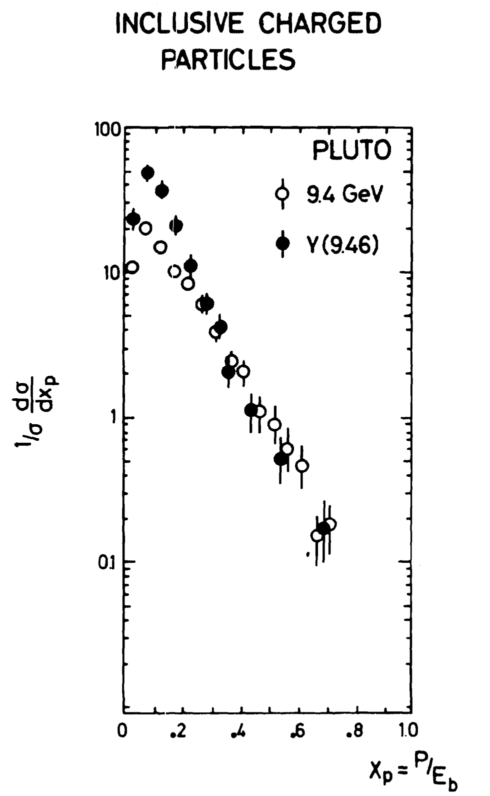

Fig. 29 Charged particle momentum spectra for the Y(9.46) and the nearby continuum.

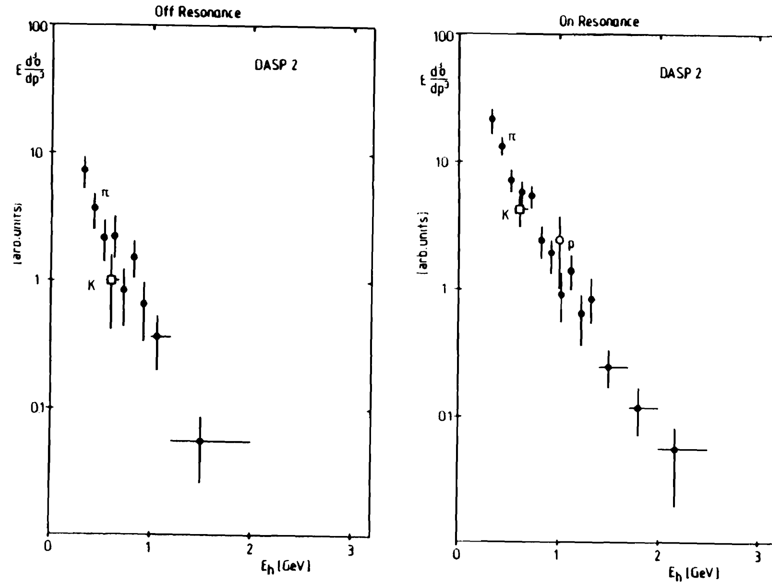

Fig. 30 The momentum spectrum of charged particles for the Y(9.46) and the continuum, for pions ⧫, kaons ⌑ and $\bar{p}$ ϕ from ref. 35.

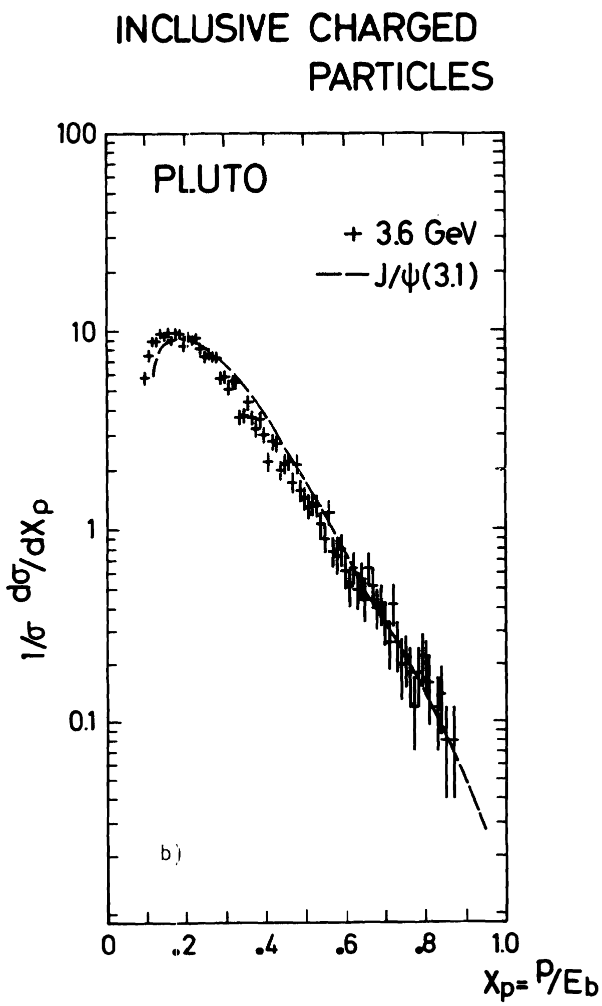

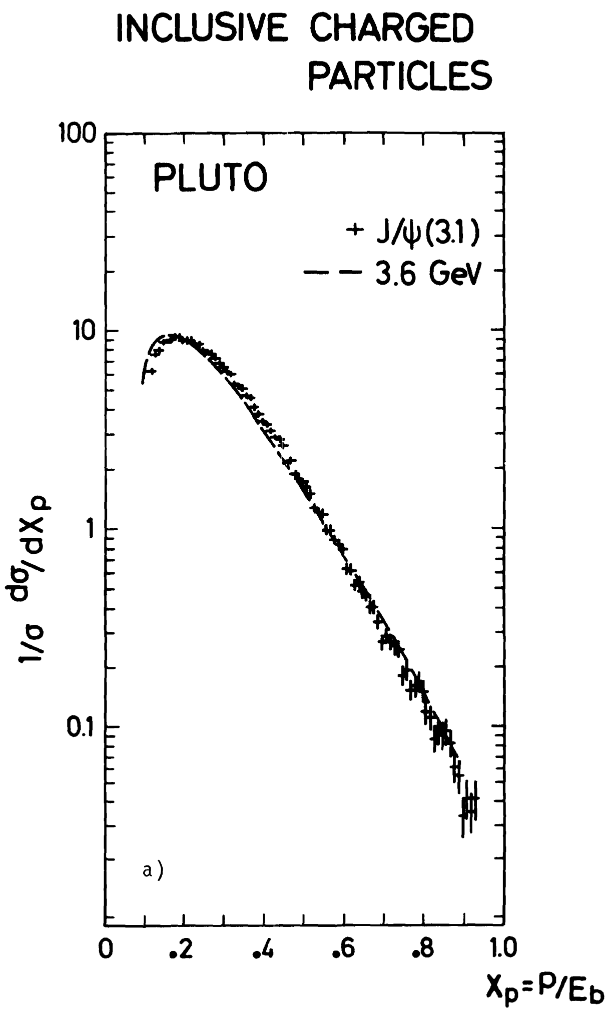

Fig. 31 Inclusive charged particle spectra
a) at the J/ψ(3.1) and
b) at 3.6 GeV.

characteristic feature of QCD. It provides asymptotically for a gluon jet more hard branches in its development and leads to the predictions (a) and (b) above.

4.1. Multiplicities and $p_\perp$

Given the existence of the three-gluon coupling qualitatively one should see a rather spectacular increase in $<n>$ going from the continuum (two-quark jets) to the top of a heavy quark-antiquark resonance, both because the softer fragmentation of the gluons and because of the development of the third jet. In case of the Υ(9.46) a change in $<n_{ch}>$ has actually been observed by the three DORIS groups. The evidence is shown in fig. 27 from DHHM and fig. 28 from DASPII. Corrected numbers are shown in table 4 from PLUTO and DHHM. The increase is significant, but not very spectacular. In

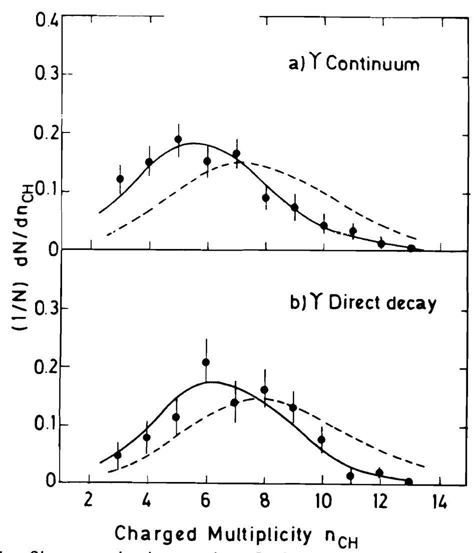

Fig. 27 Observed charged multiplicity
a) near and
b) at the Υ(9.46).
For comparison the result of the two-jet and three-jet calculations from ref. 27.

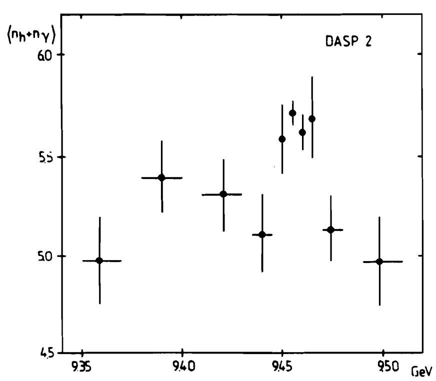

Fig. 28 Observed particle multiplicity in the Υ(9.46) region from ref. 35.

the framework of the three-gluon model, assuming no difference in the gluon jet and the quark jet multiplicities from the average energy of the three different gluon jets (see fig. 8) one gets

$$<n_{ch}> \Upsilon(9.46) = \frac{1}{2} \sum_i n_{ch} (2 E_i)$$

where n_{ch} $(2 E_i)$ is the quark jet multiplicity at two times the gluon energies E_i. Evaluated using the data compiled in ref. 34 one expects $<n_{ch}>$ Υ(9.46) = 7.6 ±0.5 in agreement with the data in table 4. The observations on Υ(9.46) are thus consistent with equal fragmentation properties of quark and gluon jets and the development of a third jet in support of the three-gluon jet decay model.

A fragmentation model for the gluon where the gluon decays to a quark pair which then fragment independently would lead to higher multiplicity (~ 10) for Υ(9.46)[36]. This option is, therefore, not supported by the multiplicity data.

Larger $p_\perp$ with respect to the gluon-jet axis will lead to a bigger $<p_\perp>_{out}$ measured against the plane of the three-gluon events compared to the prediction based on the $p_\perp$ of quark jets. The numbers obtained are 0.132 ±0.003 for the Υ(9.46) data and 0.140 ±0.006 for the gluon model assuming quark-jet properties for the gluon[25]. No increase over the quark-jet value is observed.

Table 4

Exp.	continuum	Υ(9.46)	Υ(9.46)/continuum	reference
DHHM	6.1 ±0.2	6.9 ±0.2	1.13	27
DASPII	5.15	5.88	1.14	35
PLUTO	6.3 ±0.4	8.0 ±0.3	1.27	25
DHHM	5.9 ±0.2	7.5 ±0.6	1.27	27
Expectation	6.2	7.6	1.23	36

4.2. Charged Particle Momentum Spectra

Since different processes for particle production on and off resonance - three-gluon jets versus two-quark jets - have been proposed a comparison of (charged) particle momentum spectra can give further details on the two processes.

The data are shown in fig. 29 and fig. 30. There are some differences seen (fig. 29) not unexpected since the multiplicities are different. The relative particle yields (fig. 30), however, do not show strong variations.

A moments analysis of charged particle spectra from heavy quarkonium decays was proposed as sensitive test for the presense of the three-gluon coupling[37]. Only two resonances, the J/ψ(3.1) and the Υ(9.46) are available so far. The measured momentum spectra at J/ψ(3.1) are shown in fig. 31a and are compared to the nearby continuum data (E_{CM} = 3.6 GeV), fig. 31b. At J/ψ(3.1) and the continuum point (3.6 GeV) are not very different while the data on and off resonance at 9.46 is certainly different, see fig. 29.

Fig. 32 shows the corrected momentum spectra from J/ψ(3.1) and Υ(9.46), they show considerable differences. A moments analysis following ref. 37 has been performed, resulting in ratios of moments for Λ = 0.5 GeV, a value preferred by inclusive lepton scattering analysis[38] the data require a Λ of ~0.7 GeV, see fig. 33.

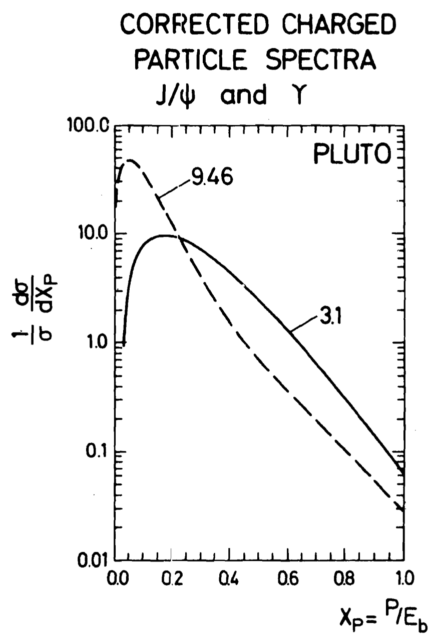

Fig. 32 Corrected data on inclusive charged particle momentum spectra on J/ψ(3.1), full line, and Υ(9.46), dashed line.

Certainly the J/ψ(3.1) resonance is not a good reference point for such an analysis. The jet structure is not at all apparent at this low energy, see for example the sphericity values in fig. 17 where both the data from the J/ψ(3.1) and the off resonance data (3.6) are still close to phase space, this means energy and momentum conservation dominate the final state once the multiplicity is fixed. At Υ(9.46) differences show up which makes it most likely a good reference point once a higher resonance (toponium) were found. Still qualitatively an inspection of fig. 33 shows the 'QCD' trend for the data. This sheds some light on the difficulties of performing a QCD analysis based on the energy dependence of particle momentum spectra since the range of validity for such an analysis is not well defined. In e^+e^- annihilation the comparison on and off resonances at least provides some basis for a judgement on this question.

4.3. Higher resonances and Three-Jet Structure

Finally a remark about a resonance at higher energies, e. g. a 'toponium' at 30 GeV. The triplicity distribution expected using the successful three-gluon model for the Υ(9.46) discussed is shown in fig. 34a together with phase space at 30 GeV in comparison to the situation at Υ(9.46), fig. 34b. The difference is impressive and indicates that very significant gluon-jet studies can be done on such a resonance.

Concerning the existence proof of three-jet events with the help of energy-flow diagrams[39] (e.g. $q\bar{q}g$ events at 30 GeV[40]) I want to show an energy-flow diagram of phase-space events at 30 GeV where triplicity has been used to give an orientation for each event, fig. 35. A "three-jet" structure is apparent. One must conclude that just the existence of a three-arm structure does not prove the three-jet structure even at this high energy, since as we see in the most trivial particle correlation the analysis can impose the three-jet structure one is looking for.

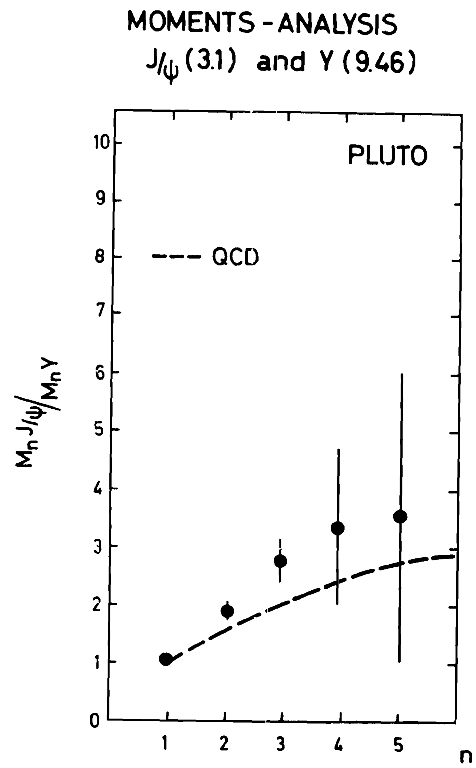

Fig. 33 The ratio of the moments of the charged particle spectra calculated from the fits to the PLUTO data shown in fig. 32. The dashed line shows the prediction of ref. 37 for Λ = 0.5 GeV.

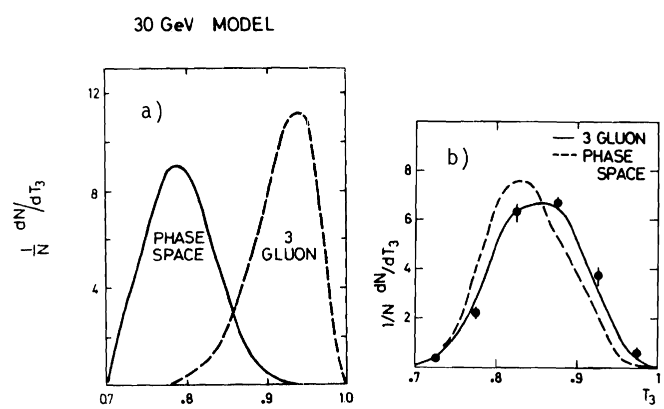

Fig. 34 A calculation of the triplicity distribution for
a) a hypothetical resonance at 30 GeV (dahsed line) as compared to phase space (full line) and
b) compared to Υ(9.46)

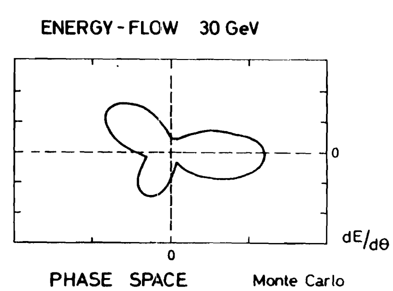

Fig. 35

Conclusions

(1) The constituent quark of the Υ(9.46) is most likely the b-quark with charge 1/3. A final proof has to come from the observation of open b-flavour and its decay modes.

(2) The hadronic decay of the Υ(9.46) is consistent with a three-jet structure and the lowest order three-gluon decay matrix element. This is based on the two- and three-jet analysis of the Υ(9.46) data.

(3) A 3 spin 0 gluon decay of the Υ(9.46) is ruled out.

(4) Gluon jets are very similar to quark jets at jet energies $\leq$ 5 GeV.

(5) A resonance at high energies (toponium family) would be a great place for definite QCD tests.

Discussion

H. Thacker
Could you show us again the kinematic limits on triplicity?

H. Meyer
The limits are $3 \cdot \sqrt{3}/8 < T < 1$

S.C.C. Ting
Your remark on your last slide is indeed correct when you are in the Υ-mass region $\sqrt{s}$ = 9. However, when you go to very high energy region with $\sqrt{s}$ > 27 GeV where the measured thrust(average) $\langle T \rangle \simeq 0.90 \pm 0.01$, which ruled out phase space completely, phase space will give a $\langle T \rangle \simeq 0.60 \pm 0.01$. With $\sqrt{s}$ > 27 GeV our energy-flow diagram in the Major-Thrust plane as presented by Dr. Newman agrees with our Monte Carlo based on QQG with an $\chi^2/DF = 50/36$. The data when compared with phase space yield an $\chi^2/DF = 282/36$; it has 10^{-6}chance of being right.

H. Meyer
Let me point out two things. First just seeing a three-arm structure does not prove the three-jet case, since even phase space does have a three-arm structure. Therefore, only a very detailed shape comparison can help deciding about the three-jet structure. Secondly I did not mean to say that phase space is an explanation of the data at very high energy in e^+e^- annihilation.

H. Newman
I would like to see the comparison of your data to a Monte Carlo model which properly includes quark-parton model ideas, which incorporates colourless gluons and a proper treatment of the fragmentation process, and which avoids the use of longitudinal phase space. The agreement between the data and the Monte Carlo seems fortuitous , given the short comings of the model.

H. Meyer
At the Υ(9.46) the jet energies are fairly low so that e. g. the Field-Feynman model does not work. A longitudinal phase space model, however does. At higher energies both models agree.

J. Rosner
Does either of the two DORIS experiments place a useful upper bound on $\Upsilon' \rightarrow \pi\pi\Upsilon$?

H. Meyer
No

J. Rosner
Any upper bound?

H. Meyer
Unfortunately, no.

Acknowledgement

I am very grateful to Fermilab for the warm hospitality extendet to me.
Many thanks to my scientific secretary, R. Wagner, for his very efficient help.
Also I want to thank H. Harari for critical and useful comments.
I want to thank Günter Flügge for very careful reading of the manuscript.

List of References

1. W. Bothe et al., IEEE Transactions in Nuclear Science NS26 (1979) 3, and DESY 79/08 (1979)
2. C.W. Darden et al., Phys. Lett. 76B (1978) 246
3. Ch. Berger et al., Phys. Lett. 76B (1978) 243
4. J.K. Bienlein et al., Phys. Lett. 78B (1978) 360
5. C.W. Darden et al., Phys. Lett. 78B (1978) 364
6. K. Ueno et al., Phys. Rev. Lett. 42 (1979) 486
7. R. Barate et al., D. PH. PE - 79 - 17
8. J.L. Rosner, Ch. Quigg and H.B. Thacker, Phys. Lett. 74B (1978) 350
9. Th. Appelquist and H. Georgi, Phys. Rev. D8 (1973) 4000;
   A. Zee, Phys. Rev. D8 (1973) 4038
10. M. Dine and J. Sapirstein, Phys. Rev. Lett. 43 (1979) 668
11. Ch. Berger et al., Phys. Lett. 86B (1979) 413 and Ch. Berger, this proceedings, page
12. D. Barber et al., Phys. Lett. 85B (1979) 463 and H. Newman, this proceedings, page
13. W. Bartel et al., DESY 79/64 (1979) and S. Orito, this proceedings, page
14. G. Wolf, this proceedings, page and DESY 79/61 (1979)
15. Ch. Berger et al., Zeitschrift für Physik C1 (1979) 343
16. C.W. Darden et al., Phys. Lett. 80B (1979) 419
17. G. Heinzelmann, talk at the XIX International Conference on High Energy Physics, Tokyo 1978, p. 263
18. R.D. Field and R.P. Feynman, Nucl. Phys. B136 (1978) 1
19. See refs. 11 - 14 and ref. 21.
20. A. Ore and J.L. Powell, Phys. Rev. 75 (1949) 1696;
    Th. Appelquist and D.H. Politzer, Phys. Rev. Lett. 34 (1975) 43
    and Phys. Rev. D12 (1975) 1404;
    K. Koller and T.F. Walsh, Phys. Lett. 72B (1977) 227;
    K. Koller and T.F. Walsh, Nucl. Phys. B140 (1978) 449;
    T.A. De Grand, Y.J. Ng, S.-H.H. Tye, Phys. Rev. D16 (1977) 3251;
    H. Fritzsch and K.H. Streng, Phys. Lett. 74B (1978) 90;
    S.J. Brodsky, T.A. De Grand, R.R. Morgan, D.G. Coyne, Phys. Lett. 73B (1978) 203;
    A. De Rujula, J. Ellis, E.G. Floratos, M.K. Gaillard, Nucl. Phys. B138 (1978) 387
21. Ch. Berger et al., Phys. Lett. 78B (1978) 176
22. J.D. Bjorken and S.J. Brodsky, Phys. Rev. D1 (1970) 1416
23. E. Farhi, Phys. Rev. Lett. 39 (1977) 1587;
    A. De Rujula et al. in ref. 20
24. C.L. Basham, L.S. Brown, S.D. Ellis, S.T. Love, Phys. Rev. D17 (1978) 2298
25. Ch. Berger et al., Phys. Lett. 83B (1979) 449
26. C.W. Darden et al., DESY Internal Report F15-78/01 (1978) unpublished
27. F.H. Heimlich et al., Phys. Lett. 86B (1979) 399
28. S. Brandt and H.D. Dahmen, Z. f. Phys. C1 (1979) 61
29. S. Brandt, talk given at the 1979 FPS Meeting in Geneva;
    see also DESY 79/43 (1979)
30. K. Koller and H. Krasemann, DESY 79/52 (1979)
31. K. Shizuya and S.H.H. Tye, Phys. Rev. Lett. 41 (1978) 787
    and Phys. Rev. D20 (1979) 1101
32. A. Ore, J.L. Powell in ref. 20
33. K. Koller, T.F. Walsh in ref. 20
34. H. Spitzer, Lecture given at the VIIth International Winter Meeting on Fundamental Physics, Segovia, Spania, February 1979,
    DESY Internal Report PLUTO-79/03 (1979)
35. C.W. Darden et al., Phys. Lett. 80B (1979) 419
36. K. Koller, T.F. Walsh in ref. 20
37. K. Koller, T.F. Walsh and P.H. Zerwas, Phys. Lett. 82B (1979) 263
38. J. Ellis, this proceedings, page
39. A. De Rujula et al., in ref. 20
40. H. Newman, this proceedings, page and D.P. Barber et al., Phys. Rev. Ltt. 43 (1979) 830